Biochimica et Biophysica Acta 1801 (2010) 1163–1174

Contents lists available at ScienceDirect

Biochimica et Biophysica Acta

journal homepage: www.elsevier.com/locate/bbalip

Cloning, mechanistic and functional analysis of a fungal sterol C24-methyltransferase implicated in brassicasterol biosynthesis

Maristela Pereira [a,1], Zhihong Song [b,1], Ludier Kesser Santos-Silva [a,1], Mathew H. Richards [b,1], Thi Thuy Minh Nguyen [b], JiaLin Liu [b], Celia Maria de Almeida Soares [a], Aline Helena da Silva Cruz [a], Kulothungan Ganapathy [b], W. David Nes [b,*]

[a] Laboratorio de Biologia Molecular, Instituto de Ciencias Biologicas, Universidade Federal de Goias, 74001-970, Goiania, Goias, Brazil
[b] Department of Chemistry and Biochemistry, Texas Tech University, Lubbock, TX 79409-1061, USA

ARTICLE INFO

Article history:
Received 22 April 2010
Received in revised form 15 June 2010
Accepted 18 June 2010
Available online 17 July 2010

Keywords:
Paracoccidiodes brasiliensis brassicasterol
Ergosterol
Membrane
Cloning
Antifungal drug
Sterol metabolome
Ergosterol evolution
Sterol methylation mechanism
Erg6p
Ergosterol biosynthesis inhibitor
Lanosterol catalysis

ABSTRACT

The first committed step in the formation of 24-alkylsterols in the ascomycetous fungus *Paracoccidiodes brasiliensis* (Pb) has been shown to involve C24-methylation of lanosterol to eburicol (24(28)-methylene-24,25-dihydro-lanosterol) on the basis of metabolite co-occurrence. A similarity-based cloning strategy was employed to obtain the cDNA clone corresponding to the sterol C24-methyltransferase (SMT) implicated in the C24-methylation reaction. The resulting catalyst, prepared as a recombinant fusion protein (His/Trx/S), was expressed in *Escherichia coli* BL21(C43) and shown to possess a substrate specificity for lanosterol and to generate a single exocyclic methylene product. The full-length cDNA has an open reading frame of 1131 base pairs and encodes a protein of 377 residues with a calculated molecular mass of 42,502 Da. The enzymatic C24-methylation gave a K_{mapp} of 38 μM and k_{catapp} of 0.14 min^{-1}. Quite unexpectedly, "plant" cycloartenol was catalyzed in high yield to 24(28)-methylene cycloartanol consistent with conformational arguments that favor that both cycloartenol and lanosterol are bound pseudoplanar in the ternary complex. Incubation of [27-^{13}C]- or [24-^{2}H]cycloartenol with *Pb*SMT and analysis of the enzyme-generated product by a combination of ^{1}H and ^{13}CNMR and mass spectroscopy established the regiospecific conversion of the *pro-Z* methyl group of the $\Delta^{24(25)}$-substrate to the *pro-R* isopropyl methyl group of the product and the migration of H24 to C25 on the *Re*-face of the original substrate double bond undergoing C24-methylation. Inhibition kinetics and products formed from the substrate analogs 25-azalanosterol (K_i 14 nM) and 26,27-dehydrolanosterol (K_i 54 μM and k_{inact} of 0.24 min^{-1}) provide direct evidence for distinct reaction channeling capitalized by structural differences in the C24- and C26-sterol acceptors. 25-Azalanosterol was a potent inhibitor of cell growth (IC_{50}, 30 nM) promoting lanosterol accumulation and 24-alkyl sterol depletion. Phylogenetic analysis of *Pb*SMT with related SMTs of diverse origin together with the results of the present study indicate that the enzyme may have a similar complement of active-site amino acid residues compared to related yeast SMTs affording monofunctional C_1-transfer behavior, yet there are sufficient differences in its overall amino acid composition and substrate-dependent partitioning pathways to group *Pb*SMT into a fourth and new class of SMT.

1. Introduction

The sterol family of natural products is characterized by a limited array of ring structures yet contain a broad range of side chain skeletal themes that originate in organisms of a photosynthetic or non-photosynthetic lineage; the phylogenetically distinct pathways start with cycloartenol (plant) or lanosterol (fungi and animals) precursors and end with the formation of Δ^5-sterols that possess a 24-H (cholesterol), β-CH_3 (ergosterol) or α-C_2H_5 group (sitosterol) (Fig. 1) [1–3]. Sterol metabolism is an ancient biochemistry that is different in humans and fungi that infect them through the rate-determining steps that control flux to the final product(s) [4,5]. Unique to fungi (and plants) is the critical slow enzyme involved with phytosterol diversity, the sterol C24-methyltransferase (SMT) [6,7]. The central role of this catalyst in the evolution of the different sterol metabolomes that occur across Kingdoms has stimulated considerable interest in the mechanism and stereochemistry of C24-methylation reactions as well as to provide a novel target for rational drug design [6–12].

Abbreviations: SMT, Sterol C24-methyltransferase; GC-MS, Gas-chromatography-mass spectroscopy; *Pb*, *Paracoccidiodes brasiliensis*; *Sc*, *Saccharomyces cerevisiae*

* Corresponding author. Tel.: +1 806 742 1673; fax: +1 806 742 1289.
E-mail address: wdavid.nes@ttu.edu (W.D. Nes).

[1] Authors contributed equally to this work.

1388-1981/$ – see front matter © 2010 Elsevier B.V. All rights reserved.
doi:10.1016/j.bbalip.2010.06.007

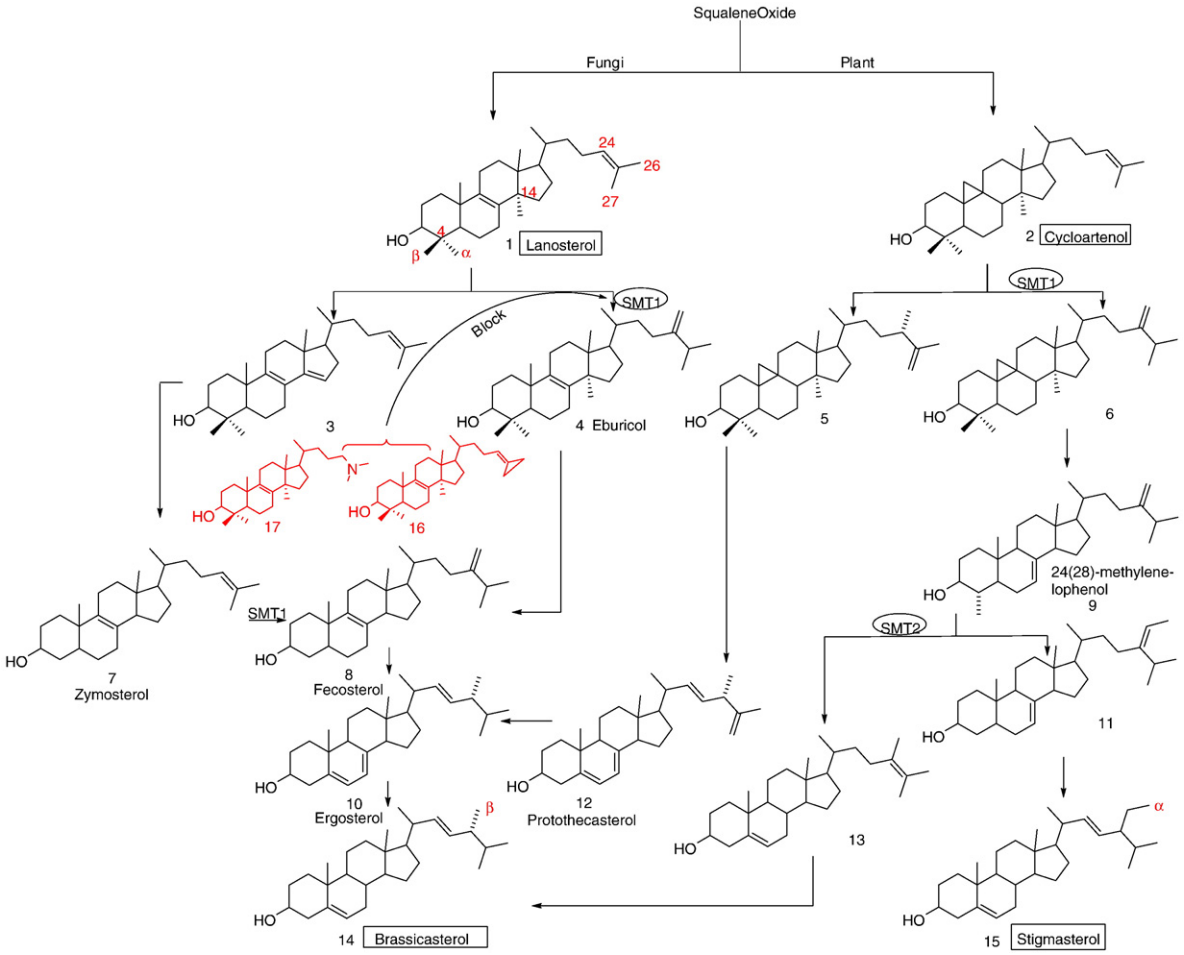

Fig. 1. Diversity of 24-alkyl sterol biosynthesis scheme. The final sterols brassicasterol and stigmasterol can be formed by different routes that occur in protozoa, fungi and plants.

Sterols play a wide range of cellular functions in fungi, as they do in animals, including that of a structural component of membranes [13], in pheromone signaling [14], as sex hormones [15] and in "sparking" cells to proliferate [16]. An important distinction for sterol usage in fungi is that these microbes must retain the 24-alkyl group in the sterol side chain for the sterol to carry out its individual functions other than that of a bulk membrane insert [17]. Fungal growth and maturation reportedly are affected by various types of sterol biosynthesis inhibitors that act on the sterol C14-demethylase (SDM) [18] or SMT enzymes [9], consistent with the essential role of these enzymes in sterol-controlled physiology. Infection too can be influenced by the sterol homeostasis of dimorphic fungi which includes *Candida albicans* and *Paracoccidiodes brasiliensis*. Notably, *P. brasiliensis*, the most frequent systemic mycoses in rural Latin America and the causative agent of paracoccidioidmycosis, is closely aligned phylogenetically to *C. albicans* [19]. The two ascomycetous fungi possess similar thermo-regulated dimorphic life cycles and sterol pathways, except that in the case of *P. brasiliensis*, the 24-alkyl sterol mixture contains significant brassicasterol (ergosta-5,22-dienol) in addition to ergosterol (ergosta-5,7-22-trienol) [20–22]. As observed by treating *C. albicans* infections with drugs targeted at ergosterol synthesis and action, *P. brasiliensis* treatment with amphotericin B and azoles led to renal side effects and emergence of resistance [19]. Therefore, there is a renewed interest and search for sterol biosynthesis inhibitors that can be developed as chemotherapeutic agents against these pathogens.

For some time, we have been interested in unearthing the molecular libraries (metabolite structure and amounts) that characterize the sterol metabolomes involved in growth and developmental regulation in order that catalyst-based sterol analogs can be designed to control flux at the rate-determining step of the pathway [1,5]. In general, SMT control governs the C24-methylation pathway with exquisite precision to generate single or multiple products; progressive inhibition of these enzymes can result in depletion of cellular 24alkyl-sterols (such as ergosterol) accompanied by growth inhibition. Several previously characterized SMTs are shown to be membrane-bound proteins with monomer $M_r = 38$ to 43 kDa of tetrameric organization, have a pH optima in the range from 6.0 to 8.8 and require AdoMet cofactor for catalysis. The catalytic competence of cloned SMTs of plant, fungal or protozoa origin is similarly slow, $k_{cat} = 0.6\ min^{-1}$, and they recognize optimal substrates with similar binding affinities, approximate $K_m = 35\ \mu M$ and $K_d = 4\ \mu M$ [1]. Comparison of the SMT primary structures demonstrated 49 to 65% sequence identity among the amino acids in them. Consistent with the significant overall sequence relatedness, these enzymes all share in four conserved substrate binding regions in the active site, three of them are sterol binding segments and one of them possess an α/β-like Rossmann-fold that serves as the AdoMet binding motif. To date, based on their substrate specificity, SMTs can be grouped into three families that relate to fungal-plant taxonomy, zymosterol (EC. 2.1.1.41), cycloartenol (EC 2.1.1.41) or 24 (28)-methylene lophenol (EC. 2.1.1.143) [1].

In contrast, much to our surprise, as described herein, upon initiating studies to establish the importance of the C24-methylation reaction involved in brassicasterol formation in *P. brasiliensis*, we discovered that the cloned *P. brasiliensis* SMT (*Pb*SMT) favored lanosterol, equally well to cycloartenol and that zymosterol, the optimal substrate for *Candida albicans* and *Saccharomyces cerevisiae* SMT (*Sc*SMT), was a poor substrate. Moreover, we found that under physiological

conditions 25-azalanosterol is a potent inhibitor of *P. brasiliensis* growth, much greater than that of the related yeasts *S. cerevisiae* and *C. albicans* [23,24]. The combination of metabolite and enzymatic results point to a new class of SMTs that prefer lanosterol as substrate and may represent a novel cellular pathway for the design of tractable sterol analogs to treat paracoccidioidmycosis.

2. Materials and methods

2.1. Pathogen and culture procedures

P. brasiliensis cells (strain Pb0, ATCC MYA-826) were grown in 1 L flasks containing 250 mL Sabouraud Dextrose Medium (SDM, Difco) for 72 h. at 36 °C. In the control, growth arrest developed after a short lag phase of 24 h; followed by a log to stationary phase growth that populated over the range from 2×10^5 cells/mL to 7×10^6 cells/mL. Cell numbers were estimated by the use of an hemocytometer (Bright-line counting chamber, Fisher). The cells were harvested and the neutral lipid fraction was isolated and processed to yield total sterols by procedures described elsewhere [25]. In a separate set of experiments, the concentration in μM of the test compound inhibiting growth to 50% of control values (IC_{50}) at growth arrest was determined from the inhibition profile. Inhibitors were dissolved in a minimum amount of dimethyl sulfoxide (<1% v/v) in the ranges from 10 nM to 1.0 μM or 1 μM to 100 μM.

2.2. Enzymes, substrates and reagents

Unless otherwise indicated, enzymes and vectors were obtained from Invitrogen. AdoMet as the iodide or chloride salts was purchased from Sigma and the sterol substrates (<98% by GLC analysis) were obtained from our collection [25 and references cited therein]. Cycloartenol samples isotopically labeled with ^2H (<98% ^2H enriched) or ^{13}C (>99% ^{13}C enriched at C27 and C26 in 8 to 2 ratio) were prepared from cycloartenol as described previously [25]. 26,27-Dehydrolanosterol and 25-azalanosterol were prepared fresh according to the reported synthetic routes [26,27]. [*methyl*-$^3H_3$]AdoMet, diluted with AdoMet iodide salt to a sp. act. of 10 μCi/μmol, was purchased from Perkin-Elmer (Waltham, MA) and [*methyl*-$^2H_3$]AdoMet (99.3% ^2H enrichment) was purchased from MSD Isotopes, Canada. All other reagents and chemicals were purchased from Fisher, Aldrich or Sigma, unless noted otherwise, and used without further purification.

2.3. Cloning full-length PbSMT

*Pb*SMT gene was cloned from an infection cDNA library of *P. brasiliensis* described by Costa et al. [28]. *Pb*SMT sequence was identified from bioinformatics resources of several databases, (http://www.ncbi.nlm.nih.gov/BLAST/ or www.tigr.org) using a BLAST search against several SMTs, including the *ERG*6 gene corresponding to the Erg6p. Degenerate primers related to the *ERG*6 gene were designed as *ERG*6-F (5′-ATAACCGAATTCATGGCGCC-3′) and *ERG*6-R (5′-ACGTGGTCGACACTTTACTC-3′) and contained engineered *Eco*RI and *Sal*I restriction sites (underlined), respectively. An 1131 bp cDNA fragment containing the complete coding region was amplified by PCR using these primers. The reaction program consisted of an initial denaturation step at 94 °C for 3 min, 30 cycles of 94 °C for 90 s, 48 °C for 2 min and 72 °C for 90 s and a final elongation at 72 °C for 10 min. The PCR product was subcloned into pGEM-T Easy vector (Promega Corp. Madison WI). The correctness of the insert was confirmed by DNA sequencing. The cDNA was excised from pGEM-T Easy vector by digestion with *Eco*RI and *Sal*I, and cloned into the *Eco*RI and *Sal*I sites pET32a (+) (Novagen, EMD Biosciences, San Diego, CA) containing one each of the S- and Trx- and His tags for antibody detection and protein purification, respectively, and transformed into the expression host *E. coli* BL21(C43) (Supplemental Fig. 1).

2.4. Heterologous expression and purification of PbSMT

*Pb*SMT gene prepared by amplification of the corresponding cDNA fragment was introduced into plasmid pET32a, and the resulting protein expressed in *E. coli* BL21 (C43) competent cells (prepared in Brazil at U.F.G.) or BL21(DE3) (prepared in the United States at T.T.U.) under control of a T7 promoter (insert size 1131 bp). For BL21 (C43) or BL21(DE3) harboring the *Pb*SMT gene construct, a single colony was inoculated into 250 mL of Luria–Bertani (LB) broth (1% tryptone, 1% NaCl and 0.5% yeast extract) (pH 7.5) supplemented with ampicillin (50 μg/mL) and 20 mM glucose and grown for 10 h at 30 °C at 200 rpm shaking.. A 20 mL aliquot of this starter culture was added to 2.8 L Erlenmeyer flasks containing 1 L of LB medium supplemented with 1 mL of the stock ampicillin. The inoculum was grown in the medium for approximately 3 h to A_{600nm} 0.5 at 30 °C, then 400 μL of 1 M isopropyl-1-thio-β-D-galactoside (IPTG) (Research Products International Corp.) was added to the culture flask and the cells further incubated for another 3 h at 30 °C with moderate shaking (150 rpm) to induce recombinant *Pb*SMT expression. The resulting cells were harvested and the pellet centrifuged at 4 °C, 10,000×*g*, 10 min. The cell paste was stored at 20 °C for short term storage or used directly for the enzyme studies. For *Pb*SMT purification, the recombinant protein was purified using the Ni-NTA resin (Invitrogen) following the manufacturer's instructions. The levels of expression, purity and size of the recombinant protein were monitored chromatographically on a 12% sodium dodecyl sulfate-polyacrylamide gel electrophoresis (SDS-PAGE) followed by Coomassie Blue or silver staining. Total protein concentrations were determined by the Bradford method with commercial reagents (Bio-Rad) using bovine γ-globulin as standard [26].

2.5. Site-directed mutagenesis of PbSMT

The QuickChange™(QC) site-directed mutagenesis kit (Stratagene) was used to produce site-specific mutations at Tyr88 (Tyr81 in the *ERG*6 nomenclature) positions of pET32a(+)-*Pb*SMT using appropriate primers. Polymerase chain reaction amplification with a specific primer was performed according to manufacturers' instruction. The plasmid was isolated using the Promega SV wizard miniprep kit and the mutation confirmed by sequencing, using the appropriate primer (T7 promoter). The mutation converting Tyr88 to leucine (Tyr88Leu) was obtained with the 45 mer primer (corresponding to codons 78–88): 5′ GCTACCGATTTCCTGGAGTATGGCTGG3′. The mutation converting Tyr88 to phenylalanine (Tyr81Phe) was obtained with the primer corresponding to codons 78–88 of 5′ GCTACCGATTTCTTCGAGTATGGCTGG. The codon corresponding to the introduced mutation is underlined. Each of the mutant constructs were transformed into *E. coli* strain B21(DE3) and the cells grown to express recombinant *Pb*SMT as described above.

2.6. Phylogenetic analyses

The *Pb*SMT deduced amino acid sequence was aligned with other SMTs available at the Pfam database and phylogenetic relationships were generated with 41 deduced complete sequences from fungi, plant and protozoa SMTs. A phylogenetic tree was constructed by multiple alignments using the CLUSTAL X program and by the neighbor-joining method visualized using the Tree View software. Robustness of branches was estimated using 100 bootstrapped replicates and indicates the percentage of times that all species appear as a monophyletic cluster.

2.7. SMT assay and inhibitors studies

Cell paste (5 g) containing the recombinant *Pb*SMT was resuspended in 30 mL of buffer (50 mM Tris–HCl, 2 mM $MgCl_2$, 2 mM

β-mercaptoethanol, and 20% glycerol (v/v), pH 7.5), and the suspension lysed by passage through a French pressure cell at 20,000 psi. Insoluble protein and cell debris were removed by centrifugation (4 °C, 100,000×*g*, 1 h), and a portion of the supernatant (approximately 25 mL) assayed. The standard assay for enzyme activity was carried out in 10 mL test tubes in final volume of 600 μL containing fixed amounts of sterol (100 μM) or the sterol concentration was varied from 5 to 150 μM in 12 μL Tween 80 (5% of an ethanol solution, v/v). Sterol packaged in Tween 80 was delivered to the bottom of the test tube and dried under a stream of nitrogen. To this film deposit was added 500 μL of 1.2 mg of soluble protein in buffer (50 mM Tris–HCl, 2 mM $MgCl_2$, 2 mM β-mercaptoethanol, and 20% glycerol (v/v), pH 7.5, 5% glycerol (v/v)). The reaction was initiated by the addition of 100 μL AdoMet (100 μM; [*methyl*-$^3H_3$]AdoMet, 0.6 μCi) and incubated for 45 min at 30 °C. The incubation mixture was terminated by addition of a solution (600 μL) of 10% methanolic-KOH. The methylated sterol products were extracted in hexane, dried and in the case of the radioactive samples analyzed by scintillation counting to determine the conversion rate.

The steady-state kinetic parameters, K_m, V_{max} and k_{cat}, established under initial velocity conditions performed on soluble protein were calculated by fitting the liquid scintillation data to the Michaelis–Menten equation using the Enzyme Kinetic Module from SSPS Inc. Inhibition of SMT using the soluble protein was assessed by graphical procedures provided by Enzyme Kinetic Module, and rate data were analyzed by linear regression analysis affording R^2 values of 0.95 to 0.97 [27]. *Pb*SMT steady-state kinetics, run under linear conditions, were performed at varied lanosterol concentrations from 5 μM to 100 μM, or at varied 25-azalanosterol concentrations from 15 nM to 100 nM, or 26,27-dehydrolanosterol concentrations from 25 to 100 μM and [*methyl*-$^3H_3$]AdoMet fixed at 100 μM. Boiled controls evidenced negligible activity with lanosterol and [*methyl*-$^3H_3$] AdoMet as substrates; in experiments with soluble *Pb*SMT approximately 500–1000 dpm were detected in assays with [*methyl*-$^3H_3$] AdoMet and no sterol; this radioactivity was background corrected in all the experimental samples. For determination of the pH, temperature, and optimal amount of enzyme, single time point assays containing 1.12 mg of soluble *Pb*SMT were incubated for 45 min at 30 °C.

2.8. Metabolite identification

For sterol quantification, GC was performed with a HP 5890 gas chromatograph fitted with a 3 ft spiral column filled with 3% SE-30 (Mesh size 100/120 on chromsorb W; Alltech, Deerfield, IL). The GC oven was maintained at 245 °C. Substrate and biomethyl products, referenced to the retention time of cholesterol (RRTc), were quantified by integration of the detector signal from 4 to 20 min. HPLC was performed using semi-preparative or analytical C_{18} TSK gel columns (Tosohaas) eluted at 1 mL/min with methanol at ambient temperature. For combined GC-MS analysis was employed, a Hewlett-Packard 6890 GC system coupled to a 5937 mass selective detector with on-column injection. Chromatography was performed on a HP-5 column (30 m×0.25 mm×0.25 mm) with the temperature program ramped from 170 °C to 280 °C at 20 °C/min with Helium carrier at 1.2 mL/min; MS was operated at an ionization voltage, 70 eV (EI) and interface temperature, 250 °C. The product distribution generated by wild-type or mutant *Pb*SMT was determined by incubating saturating levels of the co-substrates with sufficiently large preparations of protein (multiple incubations with 5–9 mg soluble protein/assay) overnight and the enzyme-generated products analyzed by GC-MS and ^1H or ^{13}CNMR. The NMR spectra were recorded in $CDCl_3$, at 500 MHz with TMS as an internal standard. Retention times in GC and HPLC are relative to the retention of cholesterol (RRTc and α_c, respectively). Product peaks were quantified by integration of peak area based internal standardization.

2.9. Time-dependent inactivation

Experiments were performed with a 100,000×*g* supernatant fraction containing the recombinant *Pb*SMT in two major steps: firstly, a pre-incubation experiment was established; to a 9 mL test tube containing analog at the test concentration (varied between 0 and 100 μM) was added 2.5 mg of total protein, 1.5 mL buffer and a fixed concentration of AdoMet (100 μM). The preparation was allowed to incubate for up to 10 min at 35 °C. Secondly, at the times indicated, aliquots (200 μL) of the pre-incubation preparation were placed in a pre-cooled (dry ice ethanol) test tube to prevent catalysis. The frozen samples were then individually thawed and filtered three times with buffer to remove excess or unbound inhibitor using Centricon YM30 (30 kDa cut off) ultrafiltration device by spinning at 5000×*g* at 4 °C in a Beckman Centrifuge. The final volume was adjusted to 500 μL with buffer. The remaining enzyme activity in each case was determined by assaying the samples at saturating concentrations of lanosterol and [*methyl* $^3H_3$]AdoMet (100 μM; 0.6 μCi) under standard assay conditions for 45 min. The logarithmic percentage of remaining enzyme activity was plotted against incubation time of enzyme–inhibitor mixture to determine the half-life ($t_{1/2}$) of inactivation. Kitz and Wilson plot was then generated using $t_{1/2}$ at each inhibitor concentration and inverse of inhibitor concentration on Sigmaplot 2001 according to the equation $-\ t_{1/2} = 0.69/k_{inact} + 0.69/k_{inact} * K_I/I$ where k_{inact} is the rate of inactivation and K_I is the concentration of inactivator that produces half maximal rate of inactivation. The point of intersection with the ordinate is the $t_{1/2}$ at saturation from which k_{inact} can be calculated while the intercept along the X-axis gives $-1/K_I$ from which K_I can be calculated [27].

For *Pb*SMT labeling, 1 mg soluble protein was treated with 100 μM of inhibitor, 100 μM of [*methyl*-$^3H_3$]AdoMet (1 μCi) in 600 μL standard buffer overnight. After dialysis and filtration (Centricon, YM10) to concentrate the protein and remove any unbound inhibitor, the protein sample was boiled in SDS buffer for 10 min prior to analysis by chromatographic separation on 12% SDS-PAGE gels. The gel was stained with Gel-Code™ (Pierce, Rockford, IL) stain solution for 20 min. The gel was saturated with fluorescent enhancer (Fluorohance, Research Product International Corp., Mt. Prospect, IL) for 30 min and then dried by a gel drier at 80 °C for 2 h. Gels were prepared for radiofluorography (Kodak XAR-5 X-ray film, Eastman Kodak company, Rochester, NY) for 4 weeks at −80 °C. Unmodified controls were included in all experiments.

3. Results

3.1. Sterol composition of control and treated cultures

Phytosterol biosynthesis consists of a series of distinct enzymatic reactions, usually involving 10 to 12 sterol genes in a given organism, that converge on a few common intermediates to form one or a mixture of 24-alkyl sterol end products. Although ergosterol is typically viewed as the major sterol synthesized in fungi, a recent study of *P. brasiliensis* revealed that ergosterol is accompanied by brassicasterol, in a precursor–product relationship [20]. From the previous GC-MS analysis of the sterol composition of *P. brasiliensis* three sterols were detected in control, lanosterol, ergosterol and brassicasterol in a ratio of 4:27:69. We reexamined the sterol composition of the fungus in order to undertake a more detailed analysis of the amounts and identities of the intermediates. Analysis of the total sterol fraction by GC-MS showed that the fungus synthesized 12 compounds of which lanosterol, ergosterol and brassicasterol make up approximately 80% of the sterol mixture (Supplemental Fig. 2, panel A) The chromatographic behavior and mass spectra of the 12 sterols detected in the *P. brasiliensis* match authentic specimens available in our steroid collection [29–31] and for compounds reported in the literature [32–34]. Lanosterol **1**,

eburicol **4**, ergosterol **10** and brassicasterol **14** (Fig. 1) were purified from the fungal sterol fraction by HPLC and analyzed by ^{1}HNMR (s, singlet, d, doublet,m, mutliplet): Compound **1**, δ, H18 (0.69, s), H19 (1.00), H21 (0.91), H26 (1.61, d), H27 (1.67, d), H30 (0.98, s), H31 (0.81, s) and H32 (0.88,s); **4**, H18 (0.69, s), H19 (1.00, s), H21 (0.92, d), H26 (1.03, d), H27 (1.03, d), H28 (4.65, d), H30 (0.98, s), H31 (0.81, s), H32 (0.88, s); **10**, H18 (0.63, s), H19 (0.95, s), H21 (1.04, d), H26 (0,82, d), H27 (0.84, d), H28 (0.92, d); H6 (5.57, m), H7 (5.37, m), H22 (5.19, m), H23 (5.18, m); 14, H18 (0.69, s), H19 (1.10, s), H21 (1.01, d), H26 (0.82, d), H27 (0.83, d), H6 (5.35, m), H22 (5.23, m), H23 (5.30, m). The chemical shifts for the side chain structures of ergosterol, brassicasterol and eburicol agree for them to possess the 24β-methyl group in **10** and **14** and exocyclic methylene group at C24 in **4** [35].

Based on these findings, we surmise that the first metabolic step in the 24-alkyl sterol synthetic pathway of *P. brasiliensis* involves the C24-methylation of lanosterol to eburicol (Supplemental Fig. 3), similar to the ergosterol pathway in the filamentous Ascomycetes *Aspergillus fumigatus* [32] and Basidiomycetes *Cryptococcus neoformans* [25]. The final product of the pathway is brassicasterol, in agreement with the natural flux of intermediates in which the sterol nucleus of Δ^8 converts to the Δ^7 to $\Delta^{5,7}$ to Δ^5-bond system [36]. In contradistinction, in the Ascomycetes *C. albicans* lanosterol is demethylated in the nucleus at C4 and C14 before C24-transalkylated of zymosterol **7** to form fecosterol **8** (Fig. 1) [36]. Interestingly, not only is the location of the C24-methylation step in 24-alkyl sterol synthesis different in the Ascomycetes, but *P. brasiliensis* may have evolved another sterol enzyme, i.e., the Δ^7-reductase, to complete the pathway to form a Δ^5-monoene as can occur in the Zygomycetes fungi, e.g., *Mortierella alpina* that accumulate cholesta-5,24-dienol (desmosterol) [37,38].

In *P. brasiliensis*, thermodynamics dictate the direction and regulatory capacity of the 24-alkyl sterol metabolic pathway with the SMT catalyzed reaction apparently operating far from equilibrium as the first committed step. It would be expected that metabolic flux through the phytosterol pathway can be controlled at the stage of sterol C24-methylation through inhibitors, allosterism or genetic control [1,6]. Indeed, inhibitors designed to interfere with *P. brasiliensis* growth and the sterol C24-methylation reaction, such as 22-piperidin-3-yl-pregnan-22(S)-3β-ol, were shown to be effective at an IC_{50} value of 250 nM resulting in the accumulation of lanosterol in the cells [20]. Thus, on mechanistic reasoning, we incubated different sterol analogs of the SMT catalyzed step with *P. brasiliensis*; 26,27-dehydrolanosterol **16** failed to inhibit fungal growth at the highest concentration of drug tested (100 μM), likely due to a lack of significant absorption into the cells. Alternatively, 25-azalanosterol **17** inhibited growth generating IC_{50} value of 35 nM ± 5 nM. The sterol composition of the treated cells at IC_{50} showed lanosterol to accumulate (<85% of total sterols, Supplemental Fig. 2, panel B), consistent with the substrate specificity of SMT predicted from the sterol pathway of control.

3.2. Cloning and sequencing of the PbSMT gene

Using a similarity-based cloning approach, the full-length cDNA sequence of the *Pb*SMT was identified and subcloned (Supplemental Figs. 1 and 4). The resulting fragment of 1131 base pairs furnished an open reading frame that encodes an apparent protein of 377 amino acids with a calculated molecular mass of 42,502 Da and theoretical p*I* of 6.08 (Fig. 2). The sequence of the putative *Pb*SMT shares significant sequence homology with SMT1 genes from ascomycetous fungi (<66% similarity) and to a lesser extent to other SMT1 and SMT2 sequences from plants and protozoa (<34% similarity) deposited in the GenBank data base. Comparison of the deduced amino acid sequence of *Pb*SMT with other members of the AdoMet-dependent methyltransferase super family showed conservation of the AdoMet binding residues observed to be in contact with AdoMet (Region II) and to contain common consensus sterol binding segments (Regions I, III and IV) (Fig. 2) in the primary structure. In addition, *Pb*SMT possessed the same set of 8 conserved signature residues that in the SCSMT upon mutation afford altered substrate specificity and product distribution [39].

3.3. Expression, purification and functional confirmation of recombinant PbSMT

Recombinant *Pb*SMT was prepared as a triple tagged fusion enzyme containing Trx, S-tag- and N-terminal His_6 sites for protein purification in *E. coli* BL21(C43). The target protein was purified to near homogeneity by Ni^{+2}-NTA agarose chromatography [40] and shown to migrate in SDS-polyacrylamide gel at M_r 60 kDa. The chromatographic behavior of this specimen is close to the calculated migration of 60.37 kDa for the fusion protein of predicted mass M_r 42,502 plus three attachments (14.33 kDa) and associated amino acids (3.53 kDa) originating at the N-terminus of the pET32a(+) vector (Fig. 3). Removal of the His-tag from the recombinant protein reduced enzyme activity therefore further work of the *Pb*SMT catalytic competence of wild-type and mutant *Pb*SMT was performed using a soluble preparation from *E. coli* BL21 (DE3).

*Pb*SMT was over-expressed as the recombinant protein in *E. coli* BL21(C43) cells. As judged by GC-MS, the soluble enzyme incubated with saturating amounts of lanosterol and AdoMet generated a single product, eburicol (24(28)-methyene-24,25-dihydro-lanosterol) in 55% yield (Fig. 4). In a similar incubation of soluble *Pb*SMT originating in BL21(DE3) cells, the catalyst generated eburicol in a 45% yield. The Michaelis constant for lanosterol was determined in the standard manner from double-reciprocal plots yielding an approximate K_m value of 38 μM ± 2 μM and V_{max} of 50 pmol/min/mg (Supplemental Fig. 5). Assay of varied concentrations of lanosterol and fixed AdoMet (100 μM) as the iodide or chloride salt with *Pb*SMT generated similar kinetic constants (data not shown). The specific activity of soluble *Pb*SMT determined for the C24-methylation reaction was established in two separate experiments from which the turnover number can be calculated using the equation $k_{cat} = V_{max}$ [SMT]. In the first experiment performed using the standard assay, the rate of lanosterol conversion to methyl product afforded a V_{max} of 50 pmol/min. In the second experiment, the amount of *Pb*SMT in the soluble protein preparation was estimated by determining the amount of "diol" product released from the *Pb*SMT-sterol complex (cf. Section 3.6) in similar fashion to the process reported for the soybean SMT2 [41]. For recombinant *Pb*SMT, the total enzyme level was determined to be approximately 7.6 μg or for the native protein to be 5.9 μg. Using the calculated M_r of *Pb*SMT of 42,505 Da and assuming the construct to be a tetramer, the yield of native enzyme in the assay is estimated to be 348 pmol. The calculated k_{cat} for the native protein is therefore 50 pmol/min/348 pmol = 0.14 min^{-1}, providing a slow turnover number similar to that reported previously for the purified SMT enzymes from several different sources [6,40,41]. The optimum pH for *Pb*SMT activity was determined to be 7.5 to 8.0, with half maximum velocities at 6.5 and 9.0 and a temperature optimum at 30 °C. The conversion rate for the soluble fraction was linear with increasing time up to 240 min in a total protein concentration of 1.4 mg/mL. These parameters are consistent with other SMTs [6].

3.4. Substrate specificity

To determine the optimal substrate for *Pb*SMT, a series of sterol acceptors that differ in the structure of the nucleus and side chain were assayed with the soluble recombinant protein. The first set of test compounds was selected based on the known substrate preferences for the three SMT isoforms, classed as SMT1fungi/protozoa, SMT1plant and SMT2 plant. Enzymatic assay of lanosterol **1** generated a K_m of 38 μM and V_{max} of 50 pmol/min which

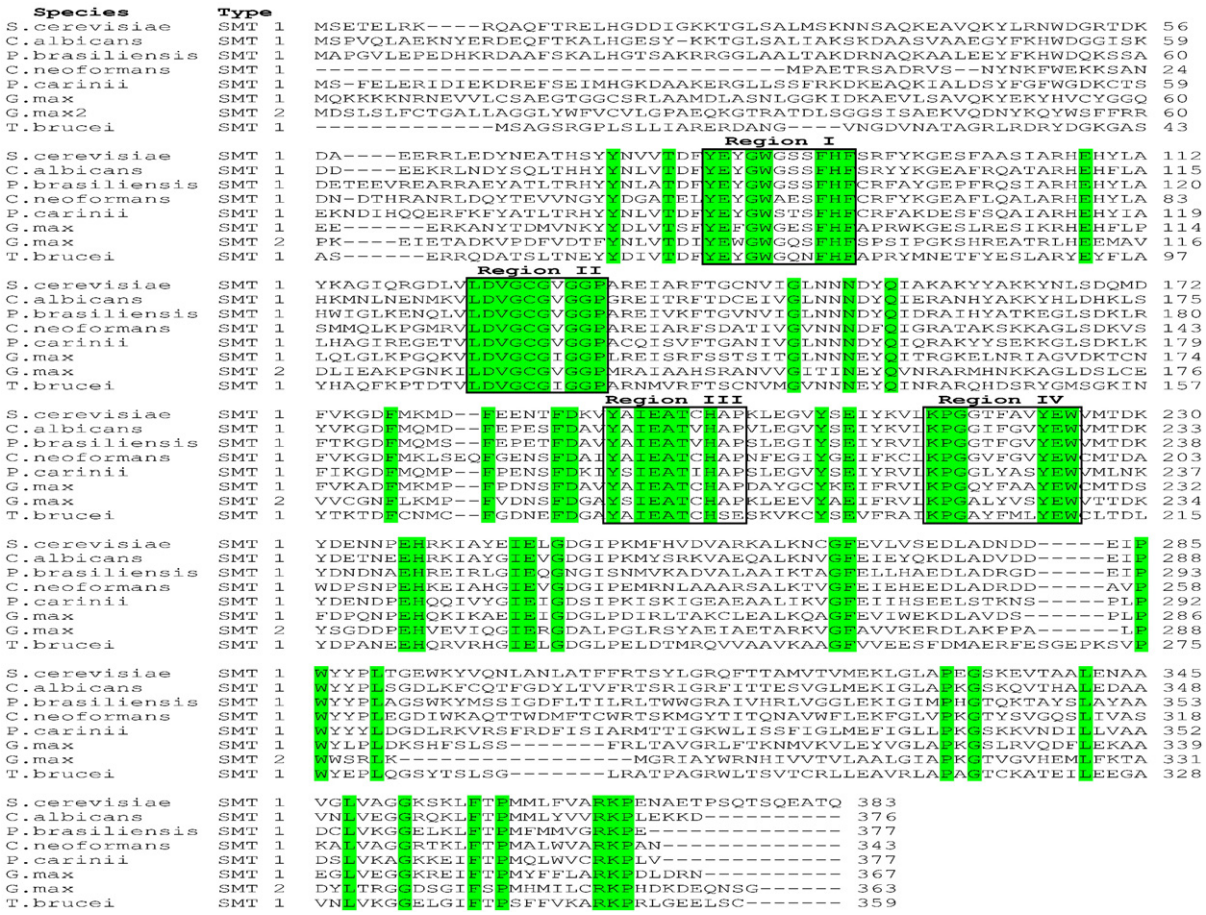

Fig. 2. Alignment of sterol C24-methyltransferase amino acid sequences (GenBank accession numbers) from *Saccharomyces cerevisiae* (NP_013706), *Candida albicans* (XP_721708), *Cryptococcus neoformans* (XP_568887), *Pneumocystis carinii* (AAK54439), *Glycine max* SMT1 (AAB04057), *Glycine max* SMT2-1 (FJ483973) and *Trypanosoma brucei* AAZ40214). Identical residues conserved in the primary structure are shaded. The sequences were aligned using Align (Informax Inc.) with defaulted parameters. The deduced substrate preference of SMT that catalyzes the first ($\Delta^{24(25)}$-substrate) or second ($\Delta^{24(28)}$-substrate) C_1-transfer reaction, SMT1 or SMT2 is reported. Sterol and AdoMet binding segments are indicated as Regions I, III, and IV and Region II, respectively.

corresponded to the optimal catalytic competence $V_{max}/K_m = 0.76$. Zymosterol **7** was a poor substrate generating a K_m 35 μM/V_{max} 2.0 pmol/min. Comparison of the properties of cycloartenol **2** and lanosterol reveals that the two substrates bind in a similar orientation in the ternary complex of the active site ($K_m = 36$ μM/$V_{max} = 48$ pmol/min). Consistent with the kinetic observations, an overnight incubation of cycloartenol with *Pb*SMT yielded a similar GC pattern of substrate-product to that of the lanosterol assay (Fig. 4).

*Pb*SMT incubation of 26,27-dehydrolanosterol **16** in which the terminal side chain carbons at C26 and C27 are fused yielded an apparent K_m 19 μM and V_{max} 6 pmol/min. Catalysis of 31-norlanosterol and 14-methyl zymosterol generated specificity constants of 35 μM/45 pmol/min and 30 μM/2 pmol/min, respectively, suggesting that neither a C4β-methyl or 14-methyl group attached to the lanosterol is harmful to activity. However, the C4α-methyl group on the lanosterol structure is crucial for optimal catalytic competence. A lack of productive binding of 24(28)-methylenelophenol **6,** fecosterol **8** or eburicol **4** (no activity) (Fig. 1) indicates that *Pb*SMT cannot perform the second alkylation step, consistent with the absence of these sterols in wild-type cells.

From these kinetic data it would appear that the natural substrate of *Pb*SMT is lanosterol, consistent with the pathway of lanosterol conversion to eburicol determined from metabolite profiling of the *P. brasiliensis* sterol metabolome. The sterols tested here possessing the lanosterol or cycloartenol frame have been considered to exist in different conformations, bent or flat and that these structural differences may explain why plant sterols cannot bind to the fungal SMTs, as reviewed in reference 6. However, their similar binding properties and other chemical data showing that they exist in solution and solid state in a pseudoplanar conformation [6] suggest that the likely shape of cycloartenol recognized by the *Pb*SMT is flat, like that of lanosterol. Accordingly, the structural feature that is paramount in SMT recognition of lanosterol and cycloartenol versus zymosterol is the C3-OH group, whose orientation in the A-ring and hydrogen-bonding ability can affect productive binding of the acceptor molecule.

3.5. Inhibition of PbSMT

In an effort to develop fungal-specific drugs that target the SMT and trap the putative 24-alkyl sterol intermediate in the C24-methylation reaction possible inhibitors, 26,27-dehydrolanosterol **16** and 25-azalanosterol **17** were constructed and fed to the fungus and independently tested with the isolated enzyme. Azasterols and related substrate analogs that possess a methylenecyclopropane structure in the sterol side chain have been used as probes of sterol biosynthesis. In the first case, they are believed to be reversible "transition state analogs" in which the protonated, ammonium form of the molecule mimics the putative carbonium ion intermediate in the methylation-reduction catalysis of the Δ^{24}-bond. In the second case, the active-site directed analog is designed to be an irreversible "mechanism-based" inhibitor specifically for the SMT [9]. Notably, under physiological conditions, these inhibitors may impair growth

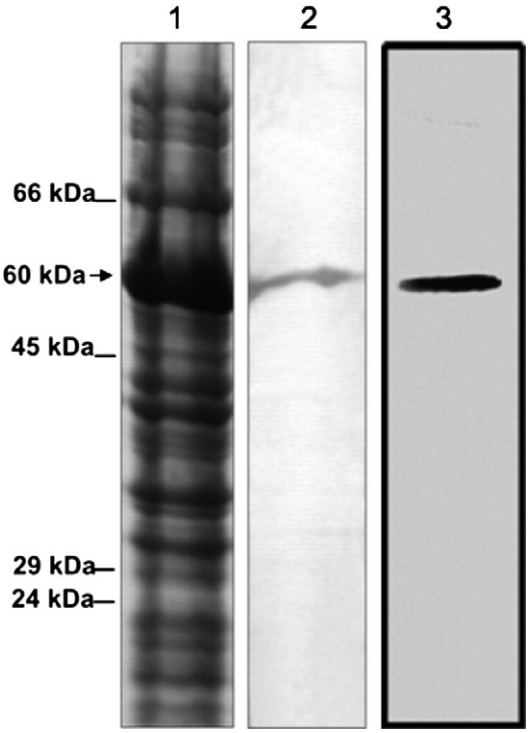

Fig. 3. SDS-PAGE analysis of recombinant *Pb*SMT purified by Ni-chromatography and corresponding fluorogram of the chemical affinity labeled soluble protein. The lanes indicated are the *E. coli* cell lysate after the addition of IPTG (lane 1), the recombinant *Pb*SMT purified by Ni-NTA resin (Lane 2) and the soluble preparation of *Pb*SMT assayed with 26,27-dehydrolanosterol paired with [*methyl*-$^3H_3$]AdoMet. The migration of protein standards (in kilodaltons, kDa) is also indicated.

by blocking enzyme action differently; through tight binding **17** or to decrease the concentration of active enzyme **16**.

Effects of 25-azalanosterol on the parameters of the Michaelis–Menten equation were determined in the presence of lanosterol or cycloartenol yielding similar competitive-type patterns relative to the test sterol and K_i values of 14 nM (Fig. 5) and 17 nM (data not shown), respectively. The kinetic behavior and resemblance of the inhibitor to the true substrate suggests tight binding in the active site but differs from it so as to be unreactive. On the other hand, if the inhibitor combines irreversibly with the *Pb*SMT the kinetic pattern can approximate that of noncompetitive inhibition since the net effect is a loss of active enzyme. Usually, this type of inhibition can be distinguished from the noncompetitive, reversible inhibition case since the reaction of inhibitor with enzyme (and/or enzyme–substrate) is not instantaneous. Instead, there is a time-dependent decrease in enzymatic activity as enzyme plus inhibitor to enzyme–inhibitor complex proceeds. The resulting covalent labeling of the enzyme should be detectable by SDS-PAGE electrophoresis and further it is expected that the enzyme inactivates such that the inactivated enzyme has 1 mol of inhibitor covalently bound per mol of active sites [40].

Incubation of increasing concentrations of **16** resulted in pseudo-first-order, time-dependent inactivation of the *Pb*SMT, as evidenced by the linear dependence of the log residual activity against time (Fig. 6). The rate of inactivation by **16** was saturable, with a maximum rate of inactivation, k_{inact}, of $0.24\ min^{-1} \pm 0.01\ min^{-1}$ ($t_{1/2} = 2.86$ min) at 0.52 μM *Pb*SMT and a K_i for **16** of 54 ± 0.02 μM. These values compare favorably with the steady-state kinetic parameters for the normal substrate lanosterol **1** ($k_{cat} = 0.14\ min^{-1} \pm 0.3\ min^{-1}$, $K_m = 38\ \mu M \pm 3\ \mu M$). Co-incubation with 10 μM of normal substrate at 50 μM and 100 μM, lanosterol, afforded protection against inactivation, generating 52% and 75% C-methylation activity, respectively. As expected, no inactivation occurred when the incubations were carried out lacking AdoMet, consistent with the absolute dependence of *Pb*SMT on the cofactor.

To examine the specificity in the presumptive covalent modification of the *Pb*SMT, soluble protein typically studied in the standard assay was treated with **16** in the presence of AdoMet diluted with catalytic amounts of [*methyl*-$^3H_3$]AdoMet (1 μCi), and the resulting protein assayed and radiofluorography (Fig. 3). Despite the fact that the soluble protein fraction contained numerous protein species as demonstrated by Coomassie staining, only a single protein was labeled and this radioactive component eluted with mobility identical to that of the purified recombinant *Pb*SMT harboring three tags (ca. 55–60 kDa).

3.6. Mechanistic rationalization of 26,27-dehydrolanosterol catalysis

The reaction of an affinity label with the *Pb*SMT involves initial formation of a reversibly bound enzyme–substrate complex, followed by catalysis to an intermediate that can be converted to a methyl product or the intermediate can be intercepted through covalent modification and hence irreversible inhibition. *Pb*SMT incubation of

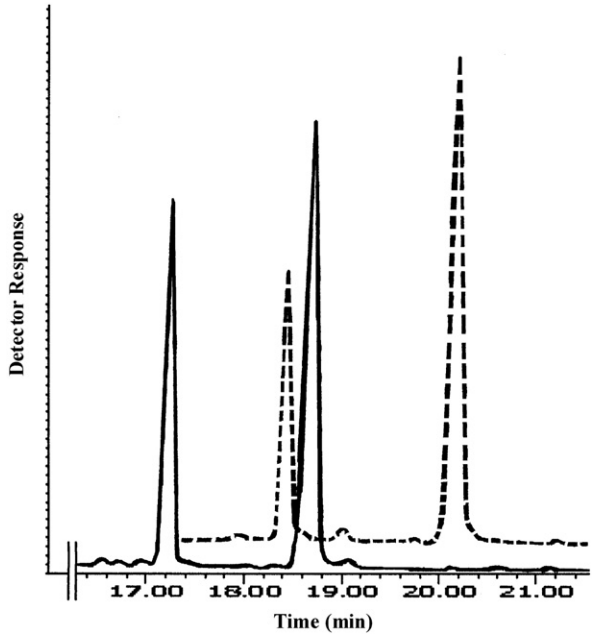

Fig. 4. GLC separation of the *Pb*SMT conversion of lanosterol to eburicol (solid line) and cycloartenol to 24(28)-methylene cycloartanol (dotted line). Product isolation and conditions for the capillary GC analysis are described under "Materials and methods".

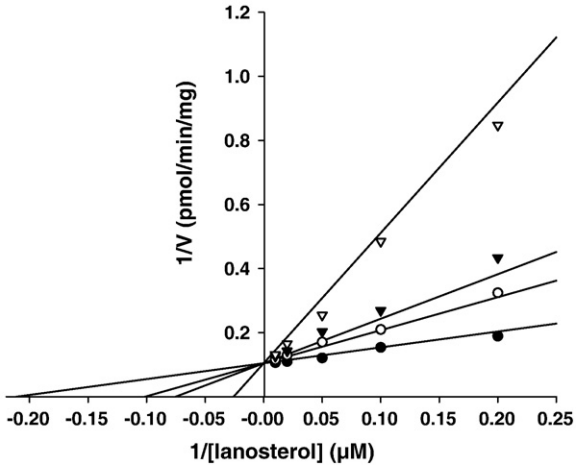

Fig. 5. Inhibition of *Pb*SMT by 25-azalanosterol. In the Lineweaver–Burk plot shown, lanosterol is the varied substrate at 0, 5 μM, 10 μM, 20 μM, 50 μM and 100 μM and AdoMet is fixed at 100 μM, and the inhibitor is varied at 0, 15 nM, 25 nM and 100 nM.

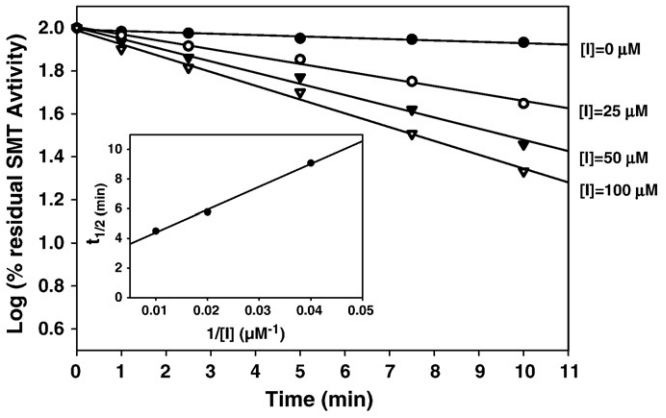

Fig. 6. Inactivation of *Pb*SMT with the mechanism-based inactivator, 26-27-dehydrolanosterol. Semi-log plots of residual activity versus time at 0 μM, 25 μM, 50 μM and 100 μM concentrations of the inhibitor. The inset shows a replot of enzyme half-life ($t_{1/2}$) for inactivation versus 1/[*I*].

lanosterol or 26,27-dehydrolanosterol can lead to distinct intermediates that convert to methylated sterol products that reflect whether the intermediate turned over ("monol") or covalently bound to the enzyme ("diol") as outlined in Fig. 7. To determine the reaction course involving these substrates catalyzed by *Pb*SMT, large-scale incubations were performed and the distribution and structures of the enzyme-generated products analyzed by HPLC, MS and NMR.

*Pb*SMT assayed with lanosterol **1** paired with [*methyl*-$^{3}H_3$]AdoMet revealed a single radioactive product in the HPLC that co-migrates with authentic eburicol (Fig. 8, panel A). *Pb*SMT assay of lanosterol paired with non-radioactive AdoMet afforded a product that in the ^{1}HNMR analysis, δ C3 (3.23, m), C18 (0.69, s), C19 (1.00,s), C21 (0.92, d), C26 (1.03 d), C27 (1.03, d), C28 (4.65, d), C31α (0.98, s), C31β (0.81, s), and C32 (0.88, s).ppm, confirmed the eburicol structure. These results show that C24-methylation of lanosterol to eburicol is regiospecific and direct thereby eliminating the possible intermediacy of a C25 cation **19** that can form hydroxylated intermediate **30** (Fig. 7, path a).

*Pb*SMT incubation of 26,27-dehydrolanosterol **16** paired with [*methyl*-$^{3}H_3$]AdoMet afforded two radioactive products, one compound elutes as a polar specimen significantly before the elution time of the substrate and a second compound elutes in the tail region of the substrate (Fig. 8, panel B.). The ratio of the two enzyme-generated products, referred to as (unknown) U-1 and U-2 is ca. 10:1, respectively. The experiment was repeated with **16** and non-radioactive AdoMet and the sterol fractions in HPLC monitored using a multiple wavelength diode-array detector to detect UV absorption for the number and type of double bonds that might be

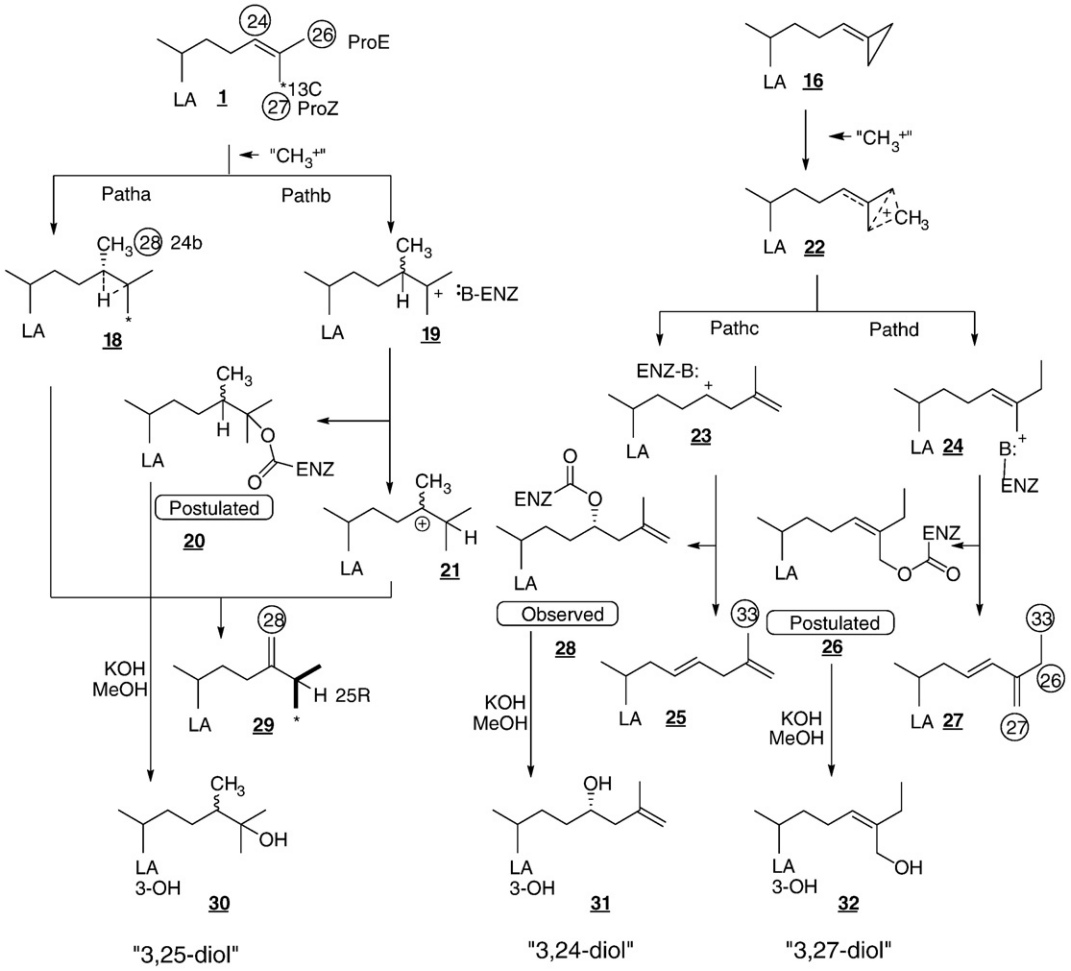

Fig. 7. Alternate pathways and mechanisms for the conversion of $\Delta^{24(25)}$-containing sterol side chains to methylated product. Formation of these monol (referring to the sterol containing a 3β-OH group) and diol (referring to the sterol containing a 3β-OH group and a second OH group in the sterol side chain) species requires distinct enzyme-bound cationic intermediates. Methyl from AdoMet addition to the sterol side chain can occur at C24 to form a C28 methyl group in structure **29** or at C26 to form a C33 methyl group in structures **25** and **27**. Interception of the enzymatic conversion of **16** to **24** and **27** can occur to inactivate the SMT; saponification of the quenched enzyme assay **31** and **32**, ligands bound in the active site of the *Pb*SMT. Note that the stereochemistry of the natural methyl product **29** is 25*R* and can be demonstrated by incubation of the relevant ^{13}C27 sterol acceptor molecule.

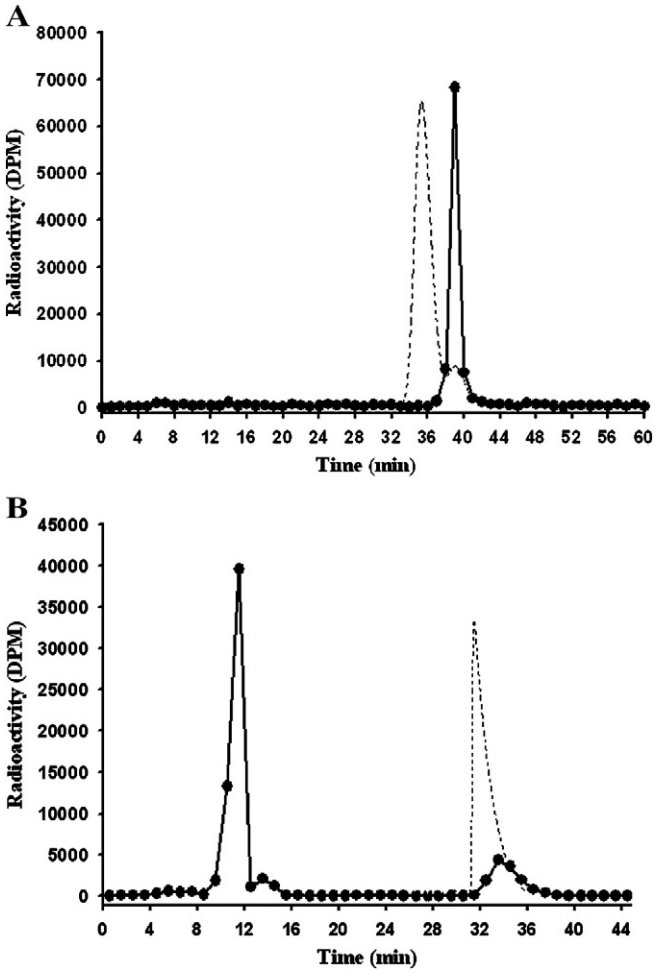

Fig. 8. HPLC chromatogram of the total sterol fraction of soluble *Pb*SMT incubated with saturating amounts of lanosterol paired with [*methyl*-$^3H_3$]AdoMet (panel A showing enzyme-generated radioactivity of 4 incubations) and saturating amounts of 26,27-dehydrolanosterol paired with [*methyl*-$^3H_3$]AdoMet (panel B showing half of the enzyme-generated radioactivity of 8 incubations) as described in the "Materials and methods" section. The dotted line shows the elution profile of the substrate and the solid line shows the elution profile of the radioactive methylated product(s). Note that in the bottom figure, the methylated diol elutes between 8 and 14 min and the methylated monol elutes between 32 and 36 min; based on the recovery of radioactivity in the fractions corresponding to the diol the *Pb*SMT k_{cat} can be determined as discussed in the Results section. Approximately 90% of the radioactivity injected into the column is recovered within the time frame of 3 to 60 min.

formed in the enzyme-generated metabolites. The relevant U-1 and U-2 compounds were recovered from the HPLC fractions and further analyzed by GC-MS (Supplemental Fig. 6) and in the case of U-2 additionally by ^{1}HNMR. For U-2, the major set of peaks in the high end of the mass spectrum were 438 (M^+), 423 (M^+-CH_3) 420 (M^+-H_20, not detected), 409 (M^+-C_2H_5, allylic cleavage of the C26–C28 system), 391 (M^+-CH_3-H_20-CH_3)), 405 (M^+-CH_3-H_20), 382 (M^+-C_4H_8, allylic cleavage thru C24/C25); the UV spectrum was bimodal with end absorption and a second peak centered at 235-240 nm indicating a Δ^8-methylated sterol with a side chain of two double bonds in conjugation. These results are consistent with U-2 to be a new C26 methyl compound **27** (Fig. 7). Incubation of **16** paired with [*methyl*-$^2H_3$]AdoMet formed U-2. The mass spectrum of this sample was composed of ions at *m/z* values of 441, 426, 409, 405, 391.The major ion of the molecular ion cluster in the high mass end of the spectrum has an *m/z* value of 441, three mass units greater than that of unlabelled U-2, consistent with the addition of three ^{2}H atoms to the sterol side chain. There is little doubt that the biosynthetically introduced ^{2}H atoms are located in the extra methyl attached to the 26-methyl group which has the structure C^2H_3 rather than the structure CH^2H_2 as would be expected for methyl attack at C24.

Incubation of **16** produced significant amounts of the polar metabolite U-1 relative to U-2 (tentatively the diol and monol metabolites reported previously using the *Sc*SMT) and much more diol than reported in the incubation of *Sc*SMT with 26,27-dehydrozymosterol [27,42,43]. The UV of U-1 possessed end absorption and the mass spectrum possessed M_r of 456 and other diagnostic ions at 441, 423, 405, 398, 383 and 365, that suggests the sterol was methylated in the side chain, contained one double bond in the side chain and contained two hydroxyl groups in the molecule, i.e. a "diol" (Supplemental Fig. 8). The ^{1}HNMR of this sample was δ C3 (3.23, m), C18 (0.69, s), C19 (1.00 s), C21 (0.93,d), C24 (5.34, m), C26 (1.68 m), C27 (3.65, m), C28 (0.894, t), C30α (0.98, s), C31β (0.81,s), C32 (0.88, s).The NMR spectrum showed the presence of a remote ethyl group (0.887, t, *j* 7.5 Hz), an olefinic proton at δ 5.34 (m) coupled to the primary alcohol group (C27 which resonated at 3.65, δ, J = 10.5 Hz) and a secondary alcohol group associated with C3 (multiplet at 3.23 ppm). The shifts of the signals for the methyl groups at C4 and C14 in the NMR spectra were consistent with retention of the lanosterol frame. The only possible structure for this new sterol is **32.** Notably, U-2 can only be recovered from the incubation mixture after treatment with methanolic-KOH, suggesting that the sterol is bound to the enzyme in an ester linkage and that the formation of the "extra" alcohol group in the sterol side chain is chemically induced during the saponification process. Further incubations of *Pb*SMT with [*methyl*-$^2H_3$]AdoMet paired with lanosterol afforded a single product of M^+ 442 amu whereas [*methyl*-$^2H_3$]AdoMet paired with 26,27-dehydrolanosterol afforded two products that contained molecular ion values at M^+ 441 amu and 459 amu, respectively. Comparison of the molecular weights of incubation products of sterol acceptor **1** and **16** paired with AdoMet versus that paired with [*methyl*-$^2H_3$]AdoMet, revealed a mass increase in the high mass end of the spectrum only [M^+ and M^+-CH_3] associated with the addition of two ^{2}H atoms in the side chain of eburicol **4** and of three ^{2}H atom increase in the side chain of **27**, respectively. The labeling studies provide support that the methyl from AdoMet introduced to the side chain of 26,27-dehydrolanosterol occurs at C26 to form a 26(33)-ethyl side chain, elongated compared to the typical phytosterols ethylated at C24(28) as in stigmasterol **15**. Taken together, the evidence indicates that the monol and diol products formed by catalysis of **16** involves partitioning of the methylated cation **22** in the direction of cation **24** which can form an alkylated enzyme with ligand structure **26** or convert to methyl product **27** after rearrangement and deprotonation of C23. This reaction path is a marked departure from the one favored by the SCSMT incubated with 26,27-dehydrozymosterol in which cation **22** proceeds down the path to cation **23** generating **25** and **31** [27].

3.7. Stereochemistry of electrophilic alkylation

The alkylating mechanism for the formation of C28 in brassicasterol involves, as a first stage, the formation of a 24(28)-methylene sterol intermediate through positional selectivity of the normal deprotonation step of the reaction (*i.e.* regioselectivity for deprotonation at C28 rather than C27 exemplified in the C-methylation reaction performed by the *P. wickerhamii* SMT, [44]) coupled to the migration of a hydrogen atom from C24 to C25. From a stereochemical point of view, this migration directed by the electrophilic alkylation attack of C24 can occur in two ways which lead to opposite configurations at C25. To probe the stereochemistry of the migration of H24 to C25, we separately incubated [24-^{2}H]cycloartenol and [^{13}C-27]cycloartenol with *Pb*SMT. Preparative incubation of *Pb*SMT with [24-^{2}H]cycloartenol generated a single product that was separated from the substrate by HPLC. MS of the enzyme-generated product gave M^+ 441 amu consistent with the methyl group and one deuterium atom addition to the sterol side chain. The 500 MHz ^{1}HNMR spectrum of the ^{2}H-labeled

C24-methylene sterol compared to that of 24(28)-methylenecycloartanol was different mainly in the chemical shifts for C26 and C-27 at 1.035 (d) and 1.22 (d) that moved downfield to δ 1.23 and 1.018 ppm due to an α-deuterium isotope effect and the signals collapsed from doublets (in the parent compound) to singlets (in the product). The retention of a single deuterium (>99%) with [24-^{2}H]cycloartenol and the detection of that deuterium at C25 in the enzyme-generated product establish that the methyl-methylene elimination at C28 and the H24 of the substrate shift to form a new stereogenic center at C25 in a stereocontrolled manner. Further *Pb*SMT incubation of [27-^{13}C] cycloartenol afforded a ^{13}C-labeled methyl product of M^{+} 441 amu (Supplemental Fig. 7, panel A). The signals for individual carbon atoms matched the spectrum previously determined in this laboratory [45]: :^{1}NMR δ ppm, 0.97 (H-18, s), 0.56 and 0.33 (H-19, d, 4.2 = endo, d, 4.2 = exo), 0.90 (H-21, d), 1.02 (H-26, dd), 1.02 (H-27, dd), 0.97 (H-30, s), 0.81 (H-31, s), 0.90 (H-32, s), 3.21 (H-3, m), 4.72, 4.67 (H-28, d, d); ^{13}CNMR (terminal side chain carbon atoms) 125 MHz δ ppm C24 (156.94), C25 (33.65), C26 (21.86), C27 (21.99) and C28 (105.90). In the ^{13}CNMR spectrum of [27-^{13}C]24(28)-methylene cycloartanol, the major enhanced signal at 21.90 ppm (Supplemental Fig.7, panel B) corresponds to C 27, therefore C25 in this specimen possesses the *R*-stereochemistry. These results indicate that *Pb*SMT catalysis of the sterol acceptor lead to a C24-methyl product in which the 1,2-hydride migration of C24 to C25 occurs specifically from the *Re*-face of the original substrate double bond undergoing transalkylation as outlined in Fig. 7, path a **1**→**18**→**29**.

3.8. Directed mutagenesis at Tyr88

The *Pb*SMT amino acid at position Tyr88 is a critical amino acid in the active sites of SMTs and corresponds to the highly conserved Tyr81 in the fungal *Sc*SMT and Tyr83 in plant *Gm*SMT primary structures. The effect of

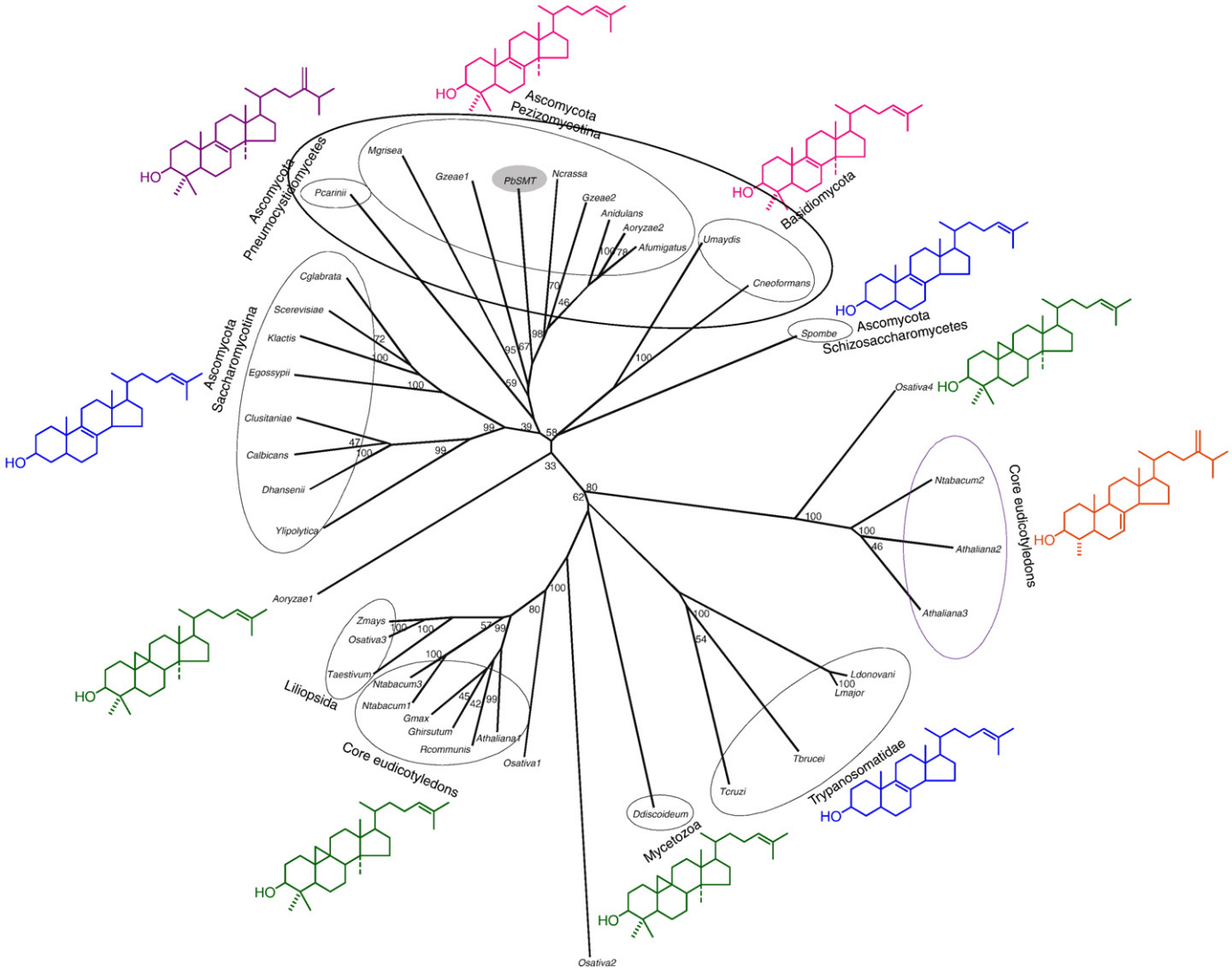

Fig. 9. Unrooted phylogenetic tree of *ERG6* genes across eukaryote Kingdoms. Complete amino acid sequences of SMTs are available in the Pfam database. The phylogenetic tree was built by the neighbor-joining method Representative organisms and GenBank accession number: *Leishmania donovani* (Q6RW42); *L. major* (Q4Q1I3); *Trypanosoma brucei* (Q4FKJ2); *T. cruzi* (Q4CMB7); *Dictyostelium discoideum* (Q54I98); *Aspergillus nidulans* (Q5AX34); *A. oryzae1* (Q2UBN2); *A. oryzae2* (Q2U0V6); *A. fumigatus* (Q4W9V1); *Gibberella zeae1* (Q4IAL8); *G. zeae2* (Q4IJ25); *Neurospora crassa* (Q9P3R1); *Candida albicans* (O74198); *C. glabrata* (Q6FRZ7); *Clavispora lusitaniae* (Q875K1); *Magnaporthe grisea* (Q5EN22); *Yarrowia lipolytica* (Q6C2D9); *Debaryomyces hansenii* (Q6BRB7); *Kluyveromyces lactis* (Q6CYB3); *Ustilago maydis* (Q4P9N1); *Saccharomyces cerevisiae* (P25087); *Pneumocystis carinii* (Q96WX4); *Eremothecium gossypii* (Q759S7); *Cryptococcus neoformans* (Q5KM39); *Schizosaccharomyces pombe* (O14321); *Arabidopsis thaliana1* (Q9LM02); *A. thaliana2* (Q39227); *A. thaliana3* (Q94JS4); *Gossypium hirsutum* (Q2QDF7); *Glycine max* (Q43445); *Ricinus communis* (O24328); *N. tabacum1* (O82434); *N. tabacum2* (O24154); *N. tabacum3* (O82720); *Triticum aestivum* (Q41586); *Oryza sativa1* (Q84M50); *O. sativa2* (Q53MP5); *O. sativa*3 (Q6ZIX2); *O. sativa4* (O82427); *Zea mays* (O49215). Robustness of branches was estimated using 100 bootstraped replicates and indicates the percentage of times that all species appear as a monophyletic cluster.

mutation on substrate binding and catalysis resulting from the substitution at Tyr-81 (Erg6p nomenclature) with leucine is a preferential change in affinity for Δ^{24}-sterols that affords alter partitioning in the direction of 24-ethyl(idene) product formation. Remarkably, when a point mutation at Tyr88 of phenylanine or leucine is introduced in the primary structure of *Pb*SMT catalytic competence is minimally affected (90% and 50% activity relative to the activity of lanosterol controls, respectively); GC-MS analysis (data not shown) of the enzyme-generated hexane-extractable lipids show a single 24-methylene sterol product. Although substrate affinity is not attenuated in the Tyr88Phe mutant, it is in the Tyr88Leu mutant, as indicated by the 50% loss in activity, suggesting that this residue in the native protein can contribute to stabilization of the active-site topography.

4. Discussion

The work described here was directed toward characterizing the sterol pathway and to establish the protein sequence and kinetic parameters of the sterol methylating enzyme necessary in the growth of *P. brasiliensis*. By examining the recombinant *Pb*SMT properties and establishing the sterol metabolome that defines brassicasterol biosynthesis, it has been possible for the first time not only to deduce the order of intermediates in sterol biosynthesis of this fungal pathogen, but also to decipher new evolutionary relationships of a crucial house keeping sterol catalyst using substrate-based cataloging. Correlation of the features giving rise to C28 and C26-methylated sterol products as well as directed mutational analysis of a key amino acid residue shown in other work to promote gain-in-function activities (acquired C_2-transfer activity) [39] revealed an unexpected influence of the activated complex architecture to guide partitioning toward enzyme inactivation in a substrate- and phyla-specific manner.

We searched the *P. brasiliensis* genome for enzyme sequences involved in sterol (http://www.broadinstitute.org/annotation/genome/paraccidioides_brasiliensis/Blast.html) biosynthesis and of the 10 ergosterol genes in the post-lanosterol pathway detailed for the *S. cerevisiae* proteome all of them have been detected. In addition, the late step Δ^7-reductase gene detected in animal systems and most recently reported in the fungus *Mortierella alpina* [46] that gives rise to the Δ^5-monoene system was also evident in the search. The proposed brassicasterol pathway shown in Supplemental Fig. 3 is much the same as the ergosterol pathway recently described in *C. neoformans* [25] but is distinct from the ergosterol-brassicasterol pathway identified in the Ascomycetes *Giberella fujikori* that proceeds from lanosterol through obtusifoliol (C4α nor-eburicol) to form fecosterol [35]. Thus there are separate pathways that can converge on the same set of 24-alkyl sterol end products.

To enable a functional genomics approach to phytosterol biosynthesis, an infection cDNA library from *P. brasiliensis* [28] was used to generate a full-length reading frame required in the cloning of *Pb*SMT. The resulting fusion protein was shown to catalyze a C_1-transfer reaction utilizing lanosterol or cycloartenol as the optimal substrate. Identification by GC-MS and NMR of the enzyme-generated products demonstrated specificity and regioselectivity of the *Pb*SMT. When investigating the apparent second-order rate constants associated with the test sterols, steady-state discrimination of 31-norlanosterol compared to zymosterol showed the former is the markedly superior substrate and that it is similar to lanosterol. Moreover, cycloartenol was accepted as an optimal substrate equal in activity to lanosterol, consistent with the product profile analyses. These results indicate that the *Pb*SMT active site is distinctly different from that of the other SMTs studied to date, including the related yeast *P. carinii* that is bifunctional (capable of C_1- and C_2-transfer activities) and catalyzes 24(28)-methyelene lanosterol producing multiple 24-ethyl(idene) lanostenols [47,48]. The NMR analyses of *Pb*SMT catalyzed cycloartenol substrates support the proposed mechanism for the C24-methylation of Δ^{24}-sterols in eukaryotes [6,7], as outlined in Fig. 7. In addition, the labeling results rule out an alternative generation of **19** such that the methyl addition from AdoMet approaches from the *Re*-face (*a*-face methylation) of the substrate double bond and firmly exclude the C24-methylation mechanism to create the 24α-methyl stereochemistry previously suggested for plant SMTs that recognize cycloartenol as substrate [49–51].

While mechanistically similar to other SMTs, the *Pb*SMT recognizes and acts on distinct substrate features and can catalyze unique partitioning that results in novel methylated products. These unusual SMT properties may be considered in the definition of *Pb*SMT into a separate and fourth family of SMTs. One implication of the sequence similarity and genomic organization of known SMT genes [1,39] is that regions of sequence conservation may correspond to functional domains and those functional domains may mediate catalysis of particular reactions common to all SMTs across kingdoms. Conversely, molecular analysis of the amino acid sequences of these SMTs coupled with the variant substrate specificity for the corresponding enzyme affords a phylogenetic tree representing the different SMT clans, in which *Pb*SMT is closely aligned to a specific Ascomycetes group as well as to the Basidiomycetes (Fig. 9). Notably, the catalytic competence carried out by SMT generates the phytosterol diversity, but how and when the requisite substrate requirements evolved and the ordering of different C-methylation pathways remains enigmatic. To this end, determination of the SMT three-dimensional structure and unearthing the roots of SMT catalysis provides an empirical approach to purse rigorous investigations of structure-guided studies to develop SMT-specific inhibitors which are currently underway.

Acknowledgements

The authors acknowledge financial support from the National Science Foundation (MCB-0920212 and MCB-0417436) and the Welch Foundation (D-1276) to WDN and the Conselho Nacional de Desenvolvimento Centifico e Tecnologico (CNPq) and International Foundation for Science (IFS), Stockholm, Sweden to MP. LKSS and AHSC are the recipients of a fellowship from the Coordenação de Aperfeiçoamento de Ensino Superior (CAPES).

Appendix A. Supplementary data

Supplementary data associated with this article can be found, in the online version, at doi:10.1016/j.bbalip.2010.06.007.

References

[1] J. Jayasimha, C.B. Bowman, J.M. Pedroza, W.D. Nes, Engineering pathway enzymes to understand the function and evolution of sterol structure and activity, Rec. Adv. Phytochem. 40 (2006) 211–251.
[2] F. Bouvier, Al. Rahier, B. Camara, Biogenesis, molecular regulation and function of plant isoprenoids, Prog. Lipid Res. 44 (2005) 357–429.
[3] P. Benveniste, Biosynthesis and accumulation of sterols, Annu. Rev. Plant Biol. 55 (2004) 429–457.
[4] J.J. Brocks, G.A. Logan, R. Buick, R.E. Summons, Archean molecular fossils and the early rise of eukaryotes, Science 285 (1999) 1033–1036.
[5] W.D. Nes, Control of sterol biosynthesis and its importance to developmental regulation and evolution, Rec. Adv. Phytochem. 24 (1990) 283–327.
[6] W.D. Nes, Sterol methyltransferase: enzymology and inhibition, Biochim. Biophys. Acta 1529 (2000) 63–88.
[7] D. Arigoni, Stereochemical studies of enzymatic C-methylation reactions, Ciba Found. Symp. 60 (1978) 243–258.
[8] J.A. Urbina, Ergosterol biosynthesis and drug development for Chagas disease, Mem. Inst. Oswaldo Cruz 104 (2009) 311–318.
[9] Z. Song, W.D. Nes, Sterol biosynthesis inhibitors: potential for transition state analogs and mechanism-based inactivators targeted at sterol methyltransferase, Lipids 42 (2007) 15–33.
[10] G. Visba, G. San-blas, J. Murgich, H. Franco, *Paracoccidiodes brasiliensis*, Paracoccidiomycosis and antifungal antibiotics, Curr. Drug Targets Infect. Disord. 5 (2005) 211–226.
[11] J. Burbiel, F. Bracher, Azasteroids as antifungals, Steroids 68 (2003) 587–594.
[12] E.S. Kaneshiro, Sterol biosynthesis in Pneumocystis: unique steps that define unique targets, Drug Resist. Updat. 5 (2002) 259–268.

[13] R. Bitmann, Has nature designed the cholesterol side chain for optimal interaction with phospholipids, Subcell. Biochem. 28 (1997) 145–171.
[14] H. Jin, J.M. McCaffery, E. Grote, Ergosterol promotes pheromone signaling and plasma membrane fusion in mating yeast, J. Cell Biol. 180 (2008) 813–826.
[15] S.A. Brunt, R. Riehl, J.C. Silver, Steroid hormone regulation of the *Achlya ambisexualis* 85-kilodalton heat shock protein, a component of the Achlya steroid receptor complex, Mol. Cell. Biol. 10 (1990) 271–281.
[16] R.J. Rodriguez, C. Low, C.D.K. Bottema, L.W. Parks, Multiple functions for sterols in *Saccharomyces cerevisiae*, Biochim. Biophys. Acta 837 (1985) 336–343.
[17] W.J. Pinto, W.R. Nes, Stereochemical specificity for sterols in *Saccharomyces cerevisiae*, J. Biol. Chem. 258 (1983) 4472–4476.
[18] J.D. Weete, Mechanism of fungal growth suppression by inhibitors of ergosterol biosynthesis, ACS Symp. Ser. 325 (1987) 268–285.
[19] G. San-Blas, G. Nino-Vega, *Paracoccidioides brasiliensis*: chemical and molecular tools for research on cell walls, antifungals, diagnosis, taxonomy, Mycopathologia 165 (2008) 183–195.
[20] G. Visba, A. Alvarez, B. Moreno, G. San-Blas, S-Adenosyl-L-methionine inhibitors Δ^{24}-sterol methyltransferase and $\Delta^{24(28)}$-sterol methylreductase as possible agents against *Pareacoccidiodes brasiliensis*, Antimicrob. Agents Chem. 47 (2003) 2966–2970.
[21] A.M. Pierce, R.B. Mueller, A.M. Unrau, A.C. Oehlschlager, Metabolism of Δ^{24}-sterols by yeast mutants blocked in removal of the C14-methyl group, Can. J. Chem. 56 (1978) 794–800.
[22] R. Kanagasabai, W. Zhou, J. Liu, T.T.M. Nguyen, P. Veeramachaneni, W.D. Nes, Disruption of ergosterol biosynthesis, growth and the morphological transition in *Candida albicans* by sterol methyltransferase inhibitors containing suflur at C25 in the sterol side chain, Lipids 39 (2004) 737–746.
[23] T.T.M. Nguyen, Influence of Inhibitors of Sterol Biosynthesis of Growth and Sterol Metabolism in *Candida albicans*, Master of Science, Texas Tech University, 2003, pp. 1–89.
[24] A.C. Oehschlager, R.H. Angus, A.M. Pierce, H.D. Pierce, R. Srinivasan, Azasterol inhibition of Δ^{24}-sterol methyltransferase in *Saccharomyces cerevisiae*, Biochemistry 23 (1984) 3582–3589.
[25] W.D. Nes, W. Zhou, K. Ganapathy, J. Liu, R. Vatsyayan, S. Chamala, K. Hernandez, M. Miranda, Sterol 24-C-methyltransferase: an enzymatic target for the disruption of ergosterol biosynthesis and homeostasis in *Cryptococcus neoformans*, Arch. Biochem. Biophys. 481 (2009) 210–218.
[26] M.M. Bradford, A rapid and sensitive method for the quantitation of microgram quantities of protein utilizing the principle of protein dye-binding, Anal. Biochem. 72 (1976) 248–254.
[27] W.D. Nes, P. Jayasimha, Z. Song, Yeast sterol C24-methyltransferase: role of highly conserved tyrosine-81 in catalytic competence studied by site-directed mutagenesis and thermodynamic analysis, Arch. Biochem. Biophys. 477 (2008) 313–323.
[28] M. Costa, C.L. Borges, A.M. Bailao, G.V. Meirelles, Y.A. Mendonca, S.F. Dantas, F.P. de Faria, M.S. Felipe, E.E. Molinari-Madlum, J. Mendes-Giannini, R.B. Fuza, W.S. Martins, M. Pereira, C.M.A. Soares, Transcriptome profiling of *Paracoccidiodes brasiliensis* yeast-phase cells recovered from infected mice brings new insight into fungal response upon host interaction, Microbiology 153 (2007) 4194–4207.
[29] W.D. Nes, G.G. Janssen, F.G. Crumley, M. Kalinowska, T. Akihisa, The structural requirements of sterols for membrane function in *Saccharomyces cerevisiae*, Arch. Biochem. Biophys. 300 (1993) 724–733.
[30] W. Zhou, G.A.M. Cross, W.D. Nes, Cholesterol import fails to prevent catalyst-based inhibition of ergosterol synthesis and cell proliferation of *Trypanosoma brucei*, J. Lipid Res. 48 (2007) 665–673.
[31] M. Venkatramesh, D. Guo, Z. Jia, W.D. Nes, Mechanism and structural requirements for transformation of substrates by the (S)-adenosyl-L methionine: $\Delta^{24(25)}$-sterol methyl transferase from *Saccharomyces cerevisiae*, Biochim. Biophys. Acta 1299 (1996) 313–324.
[32] L. Alcazar-Fuoli, E. Mellado, G. Garcia-Effron, J.F. Lopez, J.O. Grimalt, J.M. Cuenca-Estrella, J.L. Rodriguez-Tudela, Ergosterol biosynthesis pathway in *Aspergillus fumigatus*, Steroids 73 (2008) 339–347.
[33] S.W. Ellis, M.E. Rose, M. Grindle, Identification of a sterol mutant of *Neurospora crassa* deficient in D14(15)-reductase activity, J. Gen. Microbiol. 137 (1991) 2627–2630.
[34] L. Mejanelle, J.F. Loez, N. Gunde-Cimerman, J.O. Grimalt, Ergosterol biosynthesis in novel melanized fungi from hypersaline environments, J. Lipid Res. 42 (2001) 352–359.
[35] W.D. Nes, P.H. Le, Evidence for separate intermediates in the biosynthesis of 24β-methylsterol end products by *Gibberella fujikuroi*, Biochim. Biophys. Acta 1042 (1990) 119–125.
[36] W.R. Nes, M.L. McKean, Biochemistry of Steroids and Other Isopentenoids, University Park Press, Baltimore, 1977, pp. 325–455.
[37] S. Shimizu, H. Kawashima, M. Wada, H. Yamada, Occurrence of a novel sterol, 24,25-methylenecholest-5-en-3β-ol in *Mortierella alpina*,1S-4, Lipids 27 (1992) 481–483.
[38] W.D. Nes, S.D. Nichols, Phytosterol biosynthesis pathway in *Mortierella alpina*, Phytochemistry 67 (2006) 1716–1721.
[39] K. Ganapathy, C.W. Jones, C.M. Stephens, R. Vatsyayan, J.M. Marshall, W.D. Nes, Molecular probing of the *Saccharomyces cerevisiae* sterol 24-C-methyltransferase reveals multiple amino acid residues involved with C2-transfer activity, Biochim. Biophys. Acta 1781 (2008) 344–351.
[40] W. Zhou, G.I. Lepesheva, M.R. Waterman, W.D. Nes, Mechanistic analysis of a multiple product sterol methyltransferase implicated in ergosterol biosynthesis from *Trypanosoma brucei*, J. Biol. Chem. 281 (2006) 6290–6296.
[41] A.K. Neelakandan, Z. Song, J. Wang, M.H. Richards, X. Wu, B. Valliyodan, H.T. Nguyen, W.D. Nes, Cloning, functional expression, and phylogenetic analysis of plant 24C-methyltransferases involved in sitosterol biosynthesis, Phytochemistry 70 (2009) 1982–1998.
[42] J.A. Marshall, W.D. Nes, Isolation and characterization of an active-site peptide from a sterol methyl transferase with a mechanism-based inhibitor, Bioorg. Med. Chem. Lett. 9 (1999) 1533–1536.
[43] W.D. Nes, J.A. Marshall, Z. Jia, T.T. Jaradat, Z. Song, P. Jayasimha, Active site mapping and substrate channeling in the sterol methyl transferase pathway, J. Biol. Chem. 277 (2002) 42549–42556.
[44] A.T. Mangla, W.D. Nes, Sterol *C*-methyl transferase from *Prototheca wickerhamii*: mechanism, sterol specificity and inhibition, Bioorg. Med. Chem. 8 (2000) 925–936.
[45] A.L. Dennis, W.D. Nes, Sterol methyl transferase. Evidence for successive *C*-methyl transfer reactions rgenerating $\Delta^{24(28)}$- and $\Delta^{25(27)}$-olefins by a single plant enzyme, Tetrahedron Letts. 43 (2002) 7017–7021.
[46] S. Zhang, E. Sakuradani, S. Shimizu, Identification of a sterol D7-reductase gene involved in desmosterol biosynthesis in *Mortierella alpina* 1S-4, Appl. Environ. Microbiol. 73 (2007) 1736–17241.
[47] E.S. Kaneshiro, J.A. Rosenfeld, M. Brasselin-Eiweida, J.R. Stringer, S.P. Keely, A.G. Smulian, J.L. Giner, The *Pneumocystis carinii* drug target S-adenosyl-L-methionine: sterol methyltransferase has a unique substrate preference, Mol. Microbiol. 44 (2002) 989–999.
[48] W. Zhou, T.T.M. Nguyen, M.S. Collins, M.T. Cushion, W.D. Nes, Evidence for multiple sterol methyltransferse pathways in *Pneumocystis carinii*, Lipids 37 (2002) 1177–1186.
[49] S. Seo, A. Uomori, Y. Yashimura, K.J. Takeda, Stereospecificity in the biosynthesis of phytosterol side chains: carbon 13 NMR signal assignments of C26 and C27, J. Amer. Chem. Soc. 105 (1983) 6343–6344.
[50] A. Rahier, J.C. Genot, F. Schuber, P. Benveniste, A.S. Narula, Inhibition of S-adenosyl-L-methionine sterol-C-24-methyltransferase by analogues of a carbocationic ion high energy intermediate. Structure activity relationships for C-25 heteroatoms (N, As, S) substituted triterpenoid derivatives, J. Biol. Chem. 259 (1984) 15215–15223.
[51] T.W. Goodwin, Biosynthesis of sterols, in: P.K. Stumpf, E.E. Conn (Eds.), The Biochemistry of Plants: A Comprehensive Treatise, vol 4, Academic Press, New York, 1980, pp. 485–507.